Molecular Crystals and Liquid Crystals
Publication details, including instructions for authors and subscription information:
http://www.tandfonline.com/loi/gmcl20

Self-Assembled Anthracene Dimers Formed in Aqueous Solution in the Presence of γ-cyclodextrin

Naoyuki Miyakawa [a], Takayuki Kiba [a] & Shin-ichiro Sato [a]
[a] Division of Biotechnology and Macromolecular Chemistry, Graduate School of Engineering, Hokkaido University, Sapporo, Japan

Version of record first published: 19 Apr 2010

To cite this article: Naoyuki Miyakawa, Takayuki Kiba & Shin-ichiro Sato (2010): Self-Assembled Anthracene Dimers Formed in Aqueous Solution in the Presence of γ-cyclodextrin, Molecular Crystals and Liquid Crystals, 520:1, 193/[469]-200/[476]

To link to this article: http://dx.doi.org/10.1080/15421400903584408

Mol. Cryst. Liq. Cryst., Vol. 520: pp. 193/[469]–200/[476], 2010
Copyright © Taylor & Francis Group, LLC
ISSN: 1542-1406 print/1563-5287 online
DOI: 10.1080/15421400903584408

Taylor & Francis
Taylor & Francis Group

Self-Assembled Anthracene Dimers Formed in Aqueous Solution in the Presence of γ-cyclodextrin

NAOYUKI MIYAKAWA, TAKAYUKI KIBA, AND
SHIN-ICHIRO SATO

Division of Biotechnology and Macromolecular Chemistry, Graduate
School of Engineering, Hokkaido University, Sapporo, Japan

We have studied the dimer formation of a series of mono- and disubstituted anthracenes (1-methylanthracene, 2-methylanthracene, 9-methylanthracene, and 9,10-dimethylanthracene) in the γ-cyclodextrin nanocavity, using electronic absorption and fluorescence spectroscopic techniques, as well as quantum chemical calculations. We have measured fluorescence spectra of anthracene derivatives in ethanol and γ-CD aqueous solution, and the excimer-like fluorescence was observed only in γ-CD aqueous solution. The fluorescence excitation spectra observed with the excimer-like fluorescence showed an exciton splitting in the $S_3 \leftarrow S_0$ electronic transition of anthracene π-electron system. This splitting indicates that a self-assembled dimer was formed in γ-CD. The structures of dimers were estimated from the exciton splitting energies with the help of Lennard-Jones potential calculations including coulombic interactions.

Keywords anthracene; cyclodextrin; dimer; fluorescence; Lennard-Jones

1. Introduction

It is well-known that some molecules behave unusually when encapsulated inside a nanometer-sized cavity. Such an encapsulation can change the physical and chemical properties of guest molecules [1–3]. Cyclodextrins (CD) are attractive host molecules providing a nanocavity [4,5]. It is a truncated cone-shaped molecule with a hydrophilic outside and a hydrophobic hollow, the diameter of which is several angstroms. Because of this unique structure, CD forms an inclusion complex with various organic molecules in aqueous solution. The CD is even useful to investigate the effects of spatial restriction because the cavity diameter varies with the number of glucose units included in CD, e.g., α-CD (six units), β-CD (seven units), and γ-CD (eight units). Molecular structures of CDs are displayed in Scheme 1a. γ-CD has been shown to accommodate two guest molecules in its large cavity [6,7]. Control of the intermolecular interactions of aromatic hydrocarbons is crucial for the exploitation of organic supramolecular semiconductors and the incorporation of single molecules into nano-engineered devices [8].

Address correspondence to Associate Prof. Shin-ichiro Sato, Graduate School of Engineering, Hokkaido University, N13 W8, Kita-Ku, Sapporo 060-8628, Japan. Tel.: +81-11-706-6607; Fax: +81-11-706-6607; E-mail: s-sato@eng.hokudai.ac.jp

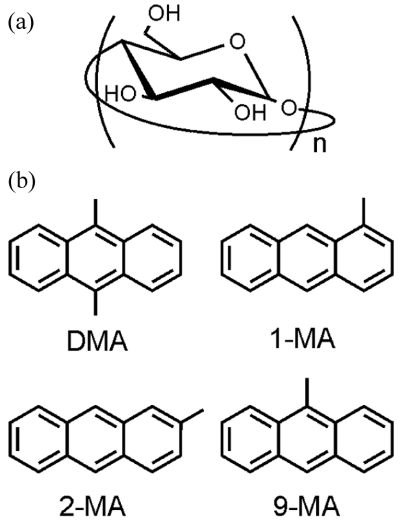

Scheme 1. (a) Molecular structures of α-CD (n = 6), β-CD (n = 7), and γ-CD (n = 8) (b) DMA, 1-MA, 2-MA, 9-MA.

In the previous study, we reported the dimer formation of 9,10-dimethylanthracene (DMA) in γ-CD nanocavity [9]. We also estimated the dimer structure of DMA on the basis of exciton energy splitting observed in fluorescence-excitation spectra. In present study, we investigated the substituent dependence of dimer structure for 1-methylanthracene, (1-MA) 2-methylanthracene (2-MA), 9-methylanthracene (9-MA). Molecular structures of DMA, 1-MA, 2-MA, and 9-MA are displayed in Scheme 1b. Dimer formation for these anthracene derivatives in γ-CD was confirmed from their absorption and fluorescence spectra. The structure of dimer was estimated from their S_3 exciton-energy splitting in the fluorescence excitation spectra with the help of LJ + coulombic potential calculations.

2. Experimental Section

9,10-dimethylanthracene, 1-methylanthracene, 2-methylanthracene, 9-methylanthracene (Aldrich, USA) and γ-CD (Kanto Kagaku, Tokyo) were used as received. A Milli-Q system (Millipore, Bedford, MA) was used for purification of water. DMA, 1-MA, 2-MA, 9-MA/γ-CD aqueous solution was prepared by mixing DMA, 1-MA, 2-MA, 9-MA/ethanol solution (200 µl; 1×10^{-3} M) with 2.5×10^{-2} M γ-CD/water solution (20 ml; 1×10^{-3} M), stirring for 12 hours.

Steady-state absorption and fluorescence spectra were measured at room temperature with a U-3010 spectrophotometer and F-4500 fluorescence spectrometer (Hitachi, Tokyo), respectively.

3. Results and Discussion and Conclusions

Absorption and fluorescence spectra of DMA, 1-MA, 2-MA, 9-MA in ethanol and in γ-CD aqueous solution at room temperature were displayed in Figure 1. The absorption spectrum of DMA in ethanol solution showed the prominent absorption

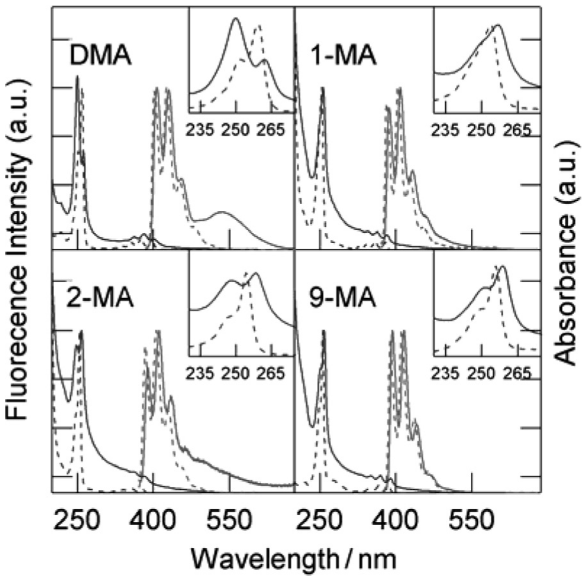

Figure 1. Absorption and fluorescence spectra of DMA, 1-MA, 2-MA, 9-MA in ethanol (broken curves) and in γ-CD water solution (solid curves). Inset: absorption spectra expanded in S_3 region.

band at 259 nm which is ascribed to the $S_0 \rightarrow S_3$ transition. The well-defined vibronic bands ranging from 300 nm to 410 nm is assigned to the $S_0 \rightarrow S_1$ transition. The absorption spectrum of 1-MA, 2-MA, and 9-MA in ethanol is very similar with that of DMA in ethanol except for their slightly shifted peak positions. The fluorescence spectrum of DMA in ethanol obtained with excitation at 376 nm (S_1 absorption) showed well-defined vibronic bands, indicating that DMA molecules exist as monomers. In a similar manner, the fluorescence spectra of 1-MA, 2-MA, and 9-MA in ethanol solution showed only monomeric S_1 fluorescence, which indicates that 1-MA, 2-MA, and 9-MA molecules also exist as monomers.

In the S_3 region of absorption spectra, peak splitting was observed for guest molecules in γ-CD aqueous solution, while the S_3 absorption showed only one peak in ethanol solution. In the case of 1-MA in γ-CD, the line width of S_3 band was broadened compared to that in ethanol. This suggested that there is also energy splitting at the S_3 absorption for 1-MA/γ-CD, although no clear splitting was observed.

The fluorescence spectrum of DMA/γ-CD obtained with excitation at 381 nm gave well-defined monomer vibronic bands (407, 430, and 456 nm) and broad excimer-like emission tailed after 500 nm. In the case of 2-MA/γ-CD, fluorescence spectrum with tailing at longer wavelength which seems to be an excimer-like emission was observed. Though very weak excimer-like emission was observed for 1-MA/γ-CD and 9-MA/γ-CD, the excitation spectra observed at 525 nm showed clear exciton splittings. These results indicate that all the guest molecules used in this study forms dimer in the presence of γ-CD in aqueous solution.

Figure 2 compares monomer- and excimer-like band detected fluorescence-excitation spectra in the S_3 region. The excitation spectra of DMA/γ-CD showed peak splitting in the region of the S_3 transition, which was very similar to the absorption spectrum, while only a single peak was observed in the monomer detected

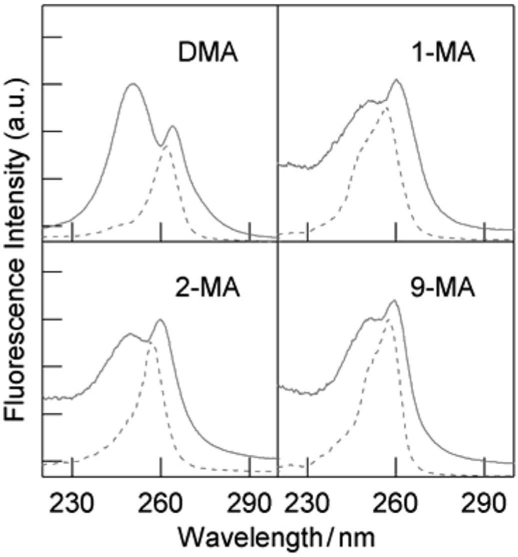

Figure 2. Fluorescence excitation spectra of DMA, 1-MA, 2-MA, 9-MA in the region of S_3 band in γ-CD water solution. The excitation spectra were recorded with the observation of monomer emission (broken curve) and with the observation of excimer-like emission (solid curve).

excitation spectrum. A similar tendency was observed for the other guest molecules. From these observations, it is concluded that the excimer-like emissions do not result from diffusive collisions of an excited guest molecules with another ground-state guest molecules, following the classic mechanism for excimer formation in bulk solvents, for which the excitation spectra of excimer species are essentially the same as those of the monomer. On the basis of the characteristic splittings of the excitation spectra observed with the excimer-like emission, the origin of the excimer-like emission can be ascribed to the excitation of the ground-state dimer species in the γ-CD nanocavity. The energy-level diagram of related states in guest molecules monomer and dimer is displayed in Figure 3.

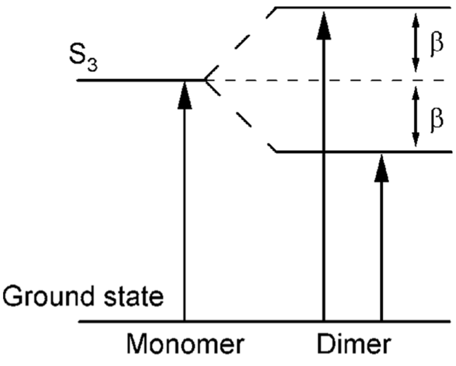

Figure 3. The energy-level diagram of related states in anthracene derivatives monomer and dimer in γ-CD.

From the S_3 peak splitting in the excitation spectra, the dipole-dipole interaction energy (β) between each monomer units was calculated as $2\beta = 2230\,\mathrm{cm}^{-1}$ (DMA), $1316\,\mathrm{cm}^{-1}$ (1-MA), $1543\,\mathrm{cm}^{-1}$ (2-MA), $1165\,\mathrm{cm}^{-1}$ (9-MA). The calculated 2β are tabulated in Table 1. From these 2β values, we calculated possible dimer structure as following. The dipole-dipole interaction energy is expressed as

$$\Delta E = 2\beta = \frac{1}{2\pi\varepsilon_0\varepsilon}\frac{e^2|\mathbf{M}|^2}{R^3}(\cos\theta_{12} - 3\cos\theta_{1R}\cos\theta_{2R}), \tag{1}$$

where e is the elementary charge, M the transition dipole moment, R the distance between the centers of chromophores, ε_0 and ε the dielectric constants of vacuum of the environment (solvents or nanocavities), respectively, θ_{12} the angle between the transition dipoles of two chromophores, $\theta_{1\mathrm{R}}$ the angle between the transition moment of the one chromophore and the distance vector, and $\theta_{2\mathrm{R}}$ the angle for the other chromophore. We assumed that the structure of the anthracene derivatives dimer will be of rotated parallel face-to-face type in the calculations. We further assumed a dimer structure in which the centers of gravity of each anthracene derivatives overlap. This assumption will be supported by the Lennard-Jones calculations in the following section. With these assumptions, Eq. (1) simplifies to

$$2\beta = \frac{1}{2\pi\varepsilon_0\varepsilon}\frac{e^2|\mathbf{M}|^2}{R^3}\cos\theta_{12}. \tag{2}$$

The transition moment can be calculated by the following equation:

$$M = \sqrt{\frac{3hf}{8\pi^2 m_e c\tilde{\nu}}}, \tag{3}$$

where m_e is the mass of an electron, c the speed of light, $\tilde{\nu}$ the wavenumber for the S_3 transition, and f the oscillator strength for the transition. The oscillator strength is given by

$$f = 4.32 \times 10^{-9} \times \frac{1}{n} \times \int \varepsilon(\tilde{\nu})d\tilde{\nu} \tag{4}$$

where n is a refractive index of solvent and $\varepsilon(\tilde{\nu})$ is a molar extinction coefficient of each anthracene derivatives. The oscillator strengths of DMA was calculated as

Table 1. Parameters of dimer orientation determined by LJ calculations

Sample	ϕ (deg.)	R (Å)	S_3 spliting (cm^{-1})	Stabilization energy ($\mathrm{kcal\,mol}^{-1}$)
1-MA	51	3.61	1316	−9.48
2-MA	45	3.59	1543	−8.97
9-MA	56	3.62	1165	−9.87
DMA	33	3.49	2230	−11.1

$f = 1.02$ from the absorption spectrum. The transition moment of DMA was calculated as $M = 1.56 \times 10^{-10}$ m, by substituting the f and $\tilde{\nu}$ values into Eq. (3). The dielectric constant inside CD was assumed to be $\varepsilon = 5.0$, which was employed by Sato *et al.* in DMA/γ-CD system [10]. The typical contour plots of DMA dimer calculation are shown in Figure 4 (left panel) for the reasonable range of R and θ_{12}. In order to determine the combination of R and θ_{12} uniquely under the condition, the intermolecular potential surface for the ground electronic state is calculated in the following section.

From the well-known Franck-Condon principle, an electronic transition of molecules takes place vertically from the ground state to an excited state. To uniquely determine the structure of the dimers which gives observed exciton splitting 2β, we calculated the potential surface of the dimers for the ground electronic state by an atom-atom Lennard-Jones (LJ) potential method including coulombic interactions [11–13]:

$$V_{LJC}(R, \theta_{12}) = \sum_{i}^{mol.1} \sum_{j}^{mol.2} \left[\frac{q_i q_j e^2}{r_{ij}} + 4\varepsilon_{ij} \left(\frac{\sigma_{ij}^{12}}{r_{ij}^{12}} - \frac{\sigma_{ij}^{6}}{r_{ij}^{6}} \right) \right], \tag{6}$$

where r_{ij} is an atom-atom distance between each monomer units, q_i (q_j) represents a charge on the i (j)th atom of each monomer units, and ε_{ij} and σ_{ij} stand for the conventional LJ parameters. For the values of ε_{ij} and σ_{ij} for the homo combinations of atoms, we used the previously reported values [11] ($\sigma_{CC} = 3.55$ Å, $\sigma_{HH} = 2.42$ Å, $\varepsilon_{CC} = 0.07$ kcal/mol, $\varepsilon_{HH} = 0.03$ kcal/mol), and the values for the hetero combinations were calculated by the combining rules as $\sigma_{AB} = (\sigma_{\mathrm{AA}}\ \sigma_{\mathrm{BB}})^{1/2}$ and $\varepsilon_{AA} = (\varepsilon_{\mathrm{AA}}\ \varepsilon_{BB})^{1/2}$.

Partial charge qs were obtained by the molecular orbital calculations (Gaussian 03W) [14] with the use of Merz Kollman scheme [15] for the each geometrically optimized anthracene-derivative monomer unit. We calculated the potential surface for each rotated face-face dimers. The right panel of Figure 4, the potential energies of DMA are plotted against θ_{12} and R. The potential energy of DMA dimer stabilized at $R = 3.6$ Å, $\theta_{12} = 42$ and 138 degree; it is noted that these two dimers are

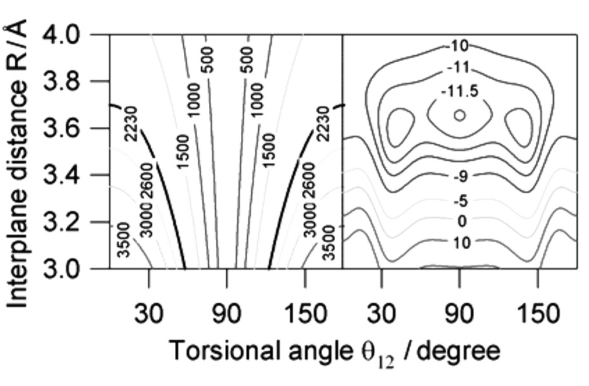

Figure 4. Left panel shows the calculated contour plots of the exciton splitting (cm^{-1}) of DMA dimer. The bold line shows the exciton splitting of 2230 cm^{-1}. Right panel shows potential energy contour plot of DMA dimer caluculated by Lennard-Jones potential with Coulombic interactions.

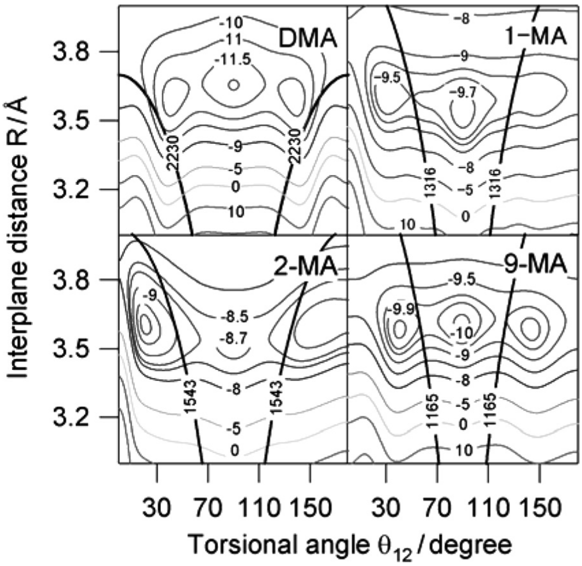

Figure 5. Potential energy contour plot caluculated by Lennard-Jones potential with Coulombic interactions. The bold line represents the exciton splitting of DMA, 1-MA, 2-MA, 9-MA.

the optical isomer each other. When $R = 3.7$ Å, the dimer stabilized at the orthogonal position. In Figure 5, shows a contour plot (solid lines) of the LJ + coulombic potential energy of all anthracene derivatives dimers investigated, overlapped with the plot (broken line) of the dipole-dipole interaction energy obtained from 2β. Based on the crossing point, at which the LJ potential minimize along the θ_{12} direction keeping the interaction energy of the observed 2β values, the plausible structure of the dimers in the barrel-type γ-CD will can be estimated. The calculated interplane distance and torsional angle of the plausible structure of dimers are summarized in Table 1. Although LJ potential map of DMA dimer was symmetric with respect to torsional angle, the other dimer was not symmetric. This is because DMA has C_2 axis, but the other dimers do not have C_2 symmetry. It was found that the tendency that the intensity of excimer fluorescence became small as the torsional angle incleased. This is because the lifetime of excimer state decreases, when the torsional angle approaches 90 degree [9]. The torsional angle of disubstituted DMA was smaller than those of monosubstituted anthracenes. This may be caused by the increased steric hinderance between DMA molecules within CD nanocavity.

4. Conclusions

We have studied the inclusion phenomena of DMA, 1-MA, 2-MA, and 9-MA in aqueous solutions in the presence of γ-CD. DMA, 1-MA, 2-MA, and 9-MA formed dimer in a γ-CD nanocavity even in the dilute solution, which was evidenced by the fluorescence and fluorescence-excitation spectra. The structure of dimers was estimated from the S_3 exciton splitting observed in the fluorescence excitation spectrum with the help of LJ + Coulombic potential calculations. In addition we could control the torsional angle of dimers by changing of the position and numbers of substituent.

Acknowledgment

This work was supported by a Grant-in-Aid for Scientific Research (C) (No. 20550001) from MEXT Japan to S.-i.S., and by Grant-in-Aid for JSPS Fellows (No. 20 · 2850) from JSPS to T.K.

References

[1] Ueno, A., Moriwaki, F., Osa, T., Hamada, F., & Murai, K. (1988). *J. Am. Chem. Soc.*, *110*, 4323.

[2] Zhou, Y.-H., Zhao, M., Sun, H., Mao, Z.-W., & Ji, L.-N. (2009). *J. Mol. Catal. A: Chem.*, *308*, 61.

[3] Chachisvilis, M., Garcia-Ochoa, I., Douhal, A., & Zewail, A. H. (1998). *Chem. Phys. Lett.*, *293*, 153.

[4] Edwin, A. C. & Ferguson, J. (1966). *J. Chem. Phys.*, *45*, 3554.

[5] Fukazawa, N., Fukumura, H., & Masuhara, H. (1994). *Chem. Phys. Lett.*, *222*, 123.

[6] Douhal, A. (2004). *Chem. Rev. (Washington, DC, U. S.)*, *104*, 1955.

[7] Takei, M., Yui, H., Hirose, Y., & Sawada, T. (2001). *J. Phys. Chem. A*, *105*, 11395.

[8] Cacialli, F., Wilson, J. S., Michels, J. J., Daniel, C., Silva, C., Friend, R. H., Severin, N., Samori, P., Rabe, J. P., O'Connell, M. J., Taylor, P. N., & Anderson, H. L. (2002). *Nat. Mater.*, *1*, 160.

[9] Sato, S.-i., Nakamura, T., Nitobe, S., Kiba, T., Hosokawa, K., Kasajima, T., Otsuka, I., Akimoto, S., & Kakuchi, T. (2006). *J. Phys. Chem. B*, *110*, 21444.

[10] Funasaki, N., Okuda, T., & Neya, S. (2001). *J. Pharm. Sci.*, *90*, 1056.

[11] Jorgensen, W. L. & Severance, D. L. (1990). *J. Am. Chem. Soc.*, *112*, 4768.

[12] Tanaka, D., Sato, S., & Kimura, K. (1998). *Chem. Phys.*, *239*, 437.

[13] Sato, S., Kojima, T., Byodo, K., Shinohara, H., Yanagihara, S., & Kimura, K. (2000). *J. Electron Spectrosc. Relat. Phenom.*, *112*, 247.

[14] Frisch, M. J., Trucks, G. W., Schlegel, H. B., Scuseria, G. E., Robb, M. A., Cheeseman, J. R., Montgomery, J. A., Vreven, T., Kudin, K. N., Burant, J. C., Millam, J. M., Iyengar, S. S., Tomasi, J., Barone, V., Mennucci, B., Cossi, M., Scalmani, G., Rega, N., Petersson, G. A., Nakatsuji, H., Hada, M., Ehara, M., Toyota, K., Fukuda, R., Hasegawa, J., Ishida, M., Nakajima, T., Honda, Y., Kitao, O., Nakai, H., Klene, M., Li, X., Knox, J. E., Hratchian, H. P., Cross, J. B., Bakken, V., Adamo, C., Jaramillo, J., Gomperts, R., Stratmann, R. E., Yazyev, O., Austin, A. J., Cammi, R., Pomelli, C., Ochterski, J. W., Ayala, P. Y., Morokuma, K., Voth, G. A., Salvador, P., Dannenberg, J. J., Zakrzewski, V. G., Dapprich, S., Daniels, A. D., Strain, M. C., Farkas, O., Malick, D. K., Rabuck, A. D., Raghavachari, K., Foresman, J. B., Ortiz, J. V., Cui, Q., Baboul, A. G., Clifford, S., Cioslowski, J., Stefanov, B. B., Liu, G., Liashenko, A., Piskorz, P., Komaromi, I., Martin, R. L., Fox, D. J., Keith, T., Laham, A., Peng, C. Y., Nanayakkara, A., Challacombe, M., Gill, P. M. W., Johnson, B., Chen, W., Wong, M. W., Gonzalez, C., & Pople, J. A. (2003). Gaussian 03, Revision D.01.

[15] Singh, U. C. & Peter, A. K. (1984). *J. Comput. Chem.*, *5*, 129.